**Supplemental Information**

# SIRPA-Inhibited, Marrow-Derived Macrophages

# Engorge, Accumulate, and Differentiate

# in Antibody-Targeted Regression of Solid Tumors

Cory M. Alvey, Kyle R. Spinler, Jerome Irianto, Charlotte R. Pfeifer, Brandon Hayes, Yuntao Xia, Sangkyun Cho, P.C.P. Dave Dingal, Jake Hsu, Lucas Smith, Manu Tewari, and Dennis E. Discher
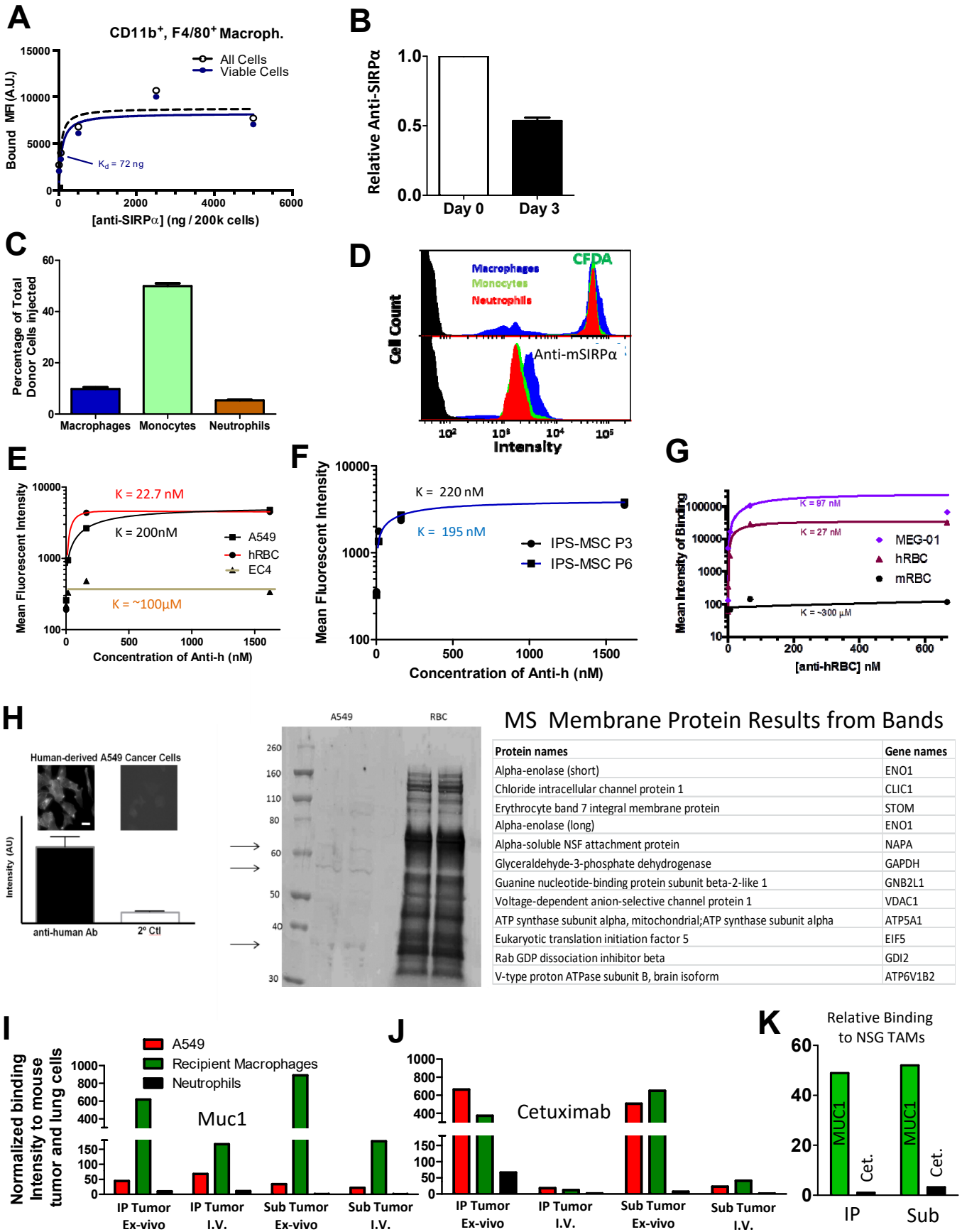
# Figure S1



**A** CD11b⁺, F4/80⁺ Macroph.
○ All Cells
● Viable Cells
$K_d = 72$ ng
Bound MFI (A.U.)
[anti-SIRPα] (ng / 200k cells)

**B** Relative Anti-SIRPα
Day 0   Day 3

**C** Percentage of Total Donor Cells injected
Macrophages   Monocytes   Neutrophils

**D** 
Macrophages
Monocytes
Neutrophils
CFDA
Anti-mSIRPα
Cell Count
Intensity

**E** Mean Fluorescent Intensity
$K = 22.7$ nM
$K = 200$nM
$K = \sim100\mu M$
A549
hRBC
EC4
Concentration of Anti-h (nM)

**F** Mean Fluorescent Intensity
$K = 220$ nM
$K = 195$ nM
IPS-MSC P3
IPS-MSC P6
Concentration of Anti-h (nM)

**G** Mean Intensity of Binding
$K = 97$ nM
$K = 27$ nM
$K = \sim300\ \mu M$
MEG-01
hRBC
mRBC
[anti-hRBC] nM

**H** Human-derived A549 Cancer Cells
Intensity (AU)
anti-human Ab   2° Ctl
A549   RBC

## MS Membrane Protein Results from Bands

| Protein names | Gene names |
|---|---|
| Alpha-enolase (short) | ENO1 |
| Chloride intracellular channel protein 1 | CLIC1 |
| Erythrocyte band 7 integral membrane protein | STOM |
| Alpha-enolase (long) | ENO1 |
| Alpha-soluble NSF attachment protein | NAPA |
| Glyceraldehyde-3-phosphate dehydrogenase | GAPDH |
| Guanine nucleotide-binding protein subunit beta-2-like 1 | GNB2L1 |
| Voltage-dependent anion-selective channel protein 1 | VDAC1 |
| ATP synthase subunit alpha, mitochondrial;ATP synthase subunit alpha | ATP5A1 |
| Eukaryotic translation initiation factor 5 | EIF5 |
| Rab GDP dissociation inhibitor beta | GDI2 |
| V-type proton ATPase subunit B, brain isoform | ATP6V1B2 |

**I** Normalized binding Intensity to mouse tumor and lung cells
A549
Recipient Macrophages
Neutrophils
Muc1
IP Tumor Ex-vivo   IP Tumor I.V.   Sub Tumor Ex-vivo   Sub Tumor I.V.

**J** Cetuximab
IP Tumor Ex-vivo   IP Tumor I.V.   Sub Tumor Ex-vivo   Sub Tumor I.V.

**K** Relative Binding to NSG TAMs
MUC1   Cet.
IP   Sub

**Figure S1. Antibody modification of NSG marrow macrophages and targeting antibody specificity** (Related to **Figure 1**)

(**A**) Affinity of anti-SIRPα for NSG macrophages. Data fit using saturation a binding model (All cells: $R^2$ = 0.73, $K_d$ = 50 ng; Viable cells: $R^2$ = 0.78, $K_d$ = 72 ng). *In vitro* phagocytosis assay using phorbol myristate acetate (PMA) treated human monocytes (THP-1) cell line and a human lung carcinoma cell line (A549, WT and CD47 KD).

(**B**) Normalized SIRPα inhibit between injections day 0 and day 3 when tumors are isolated. Approximately 53% of SIRPα inhibition remained on macrophages on day 3 (n = 3).

(**C**) Immune cells makeup of engineered NSG mouse marrow cells before injections into tumor bearing mice. Together macrophages, monocytes, and neutrophils consist of 65% of the marrow injected (n=3).

(**D**) Representative histogram of flow data from CFDA stained and anti-mSIRPα engineered NSG mouse marrow cells.

(**E and F**) Binding curve for anti-hum against hRBC, A549, EC4s, and IPS-MSC of different passage number. Each point is composed of the average intensity of 10,000 cells for each.

(**G**) Flow cytometry (gray=isotype control; black=MEG-01) of 67 nM Ab binding to MEG-01 cells. Fitting parameters indicate that when B is similar for mRBC and hRBC K for mRBC >> hRBC indicating weak affinity to mRBC. Mixing human and mouse RBCs did not affect binding to either species. Model: $Y=A+B*X/(K+X)$; hRBC: A=80, B=35524, K=26.5nM, $R^2$=0.97; mRBC: A=80, B=14210, K=323427nM, $R^2$=0.22; MEG-01: A=80, B=262480, K=97nM, $R^2$=0.99.

(**H**) Verification of anti-hum binding to A549 cells, immunofluorescence and Western blot. Immunofluorescence confirms anti-human antibody binding (left) to A549 *in vitro* compared to secondary antibody only control (right) (scale bar = 10 μm). Images have been adjusted to allow visualization of cells in control image. Bar graph below the images reflects true fluorescence of each unaltered image. The blot shows three main bands with several lower intensity bands which anti-hum binds to. Shown are possible surface proteins identified by mass spectrometry that correspond to the molecular weight from the 3 most intense bands.

(**I-J**) Binding of systemically injected anti-hMUC1 and Cetuximab antibody into NSG mice bearing 8 wk old tdTom A549 tumors. Antibody could circulate for 3 hours then the mouse was then sacrificed, tumors isolated, disaggregated, and split into two samples. One sample was stained for targeting antibody and the other was directly incubated with anti-MUC1 or Cetuximab (*ex vivo*) to ensure specific binding and to test non-specific binding. After direct incubation, samples were then stained for targeting antibodies.

(**K**) Normalized NSG TAM binding data from subcutaneous and intraperitoneal tdTom A549 tumors of anti-MUC1 and Cetuximab. 10ug of each antibody was systemically injected and 3 hours later the mouse was sacrificed, tumor tissue stained, and analyzed by flow cytometry.
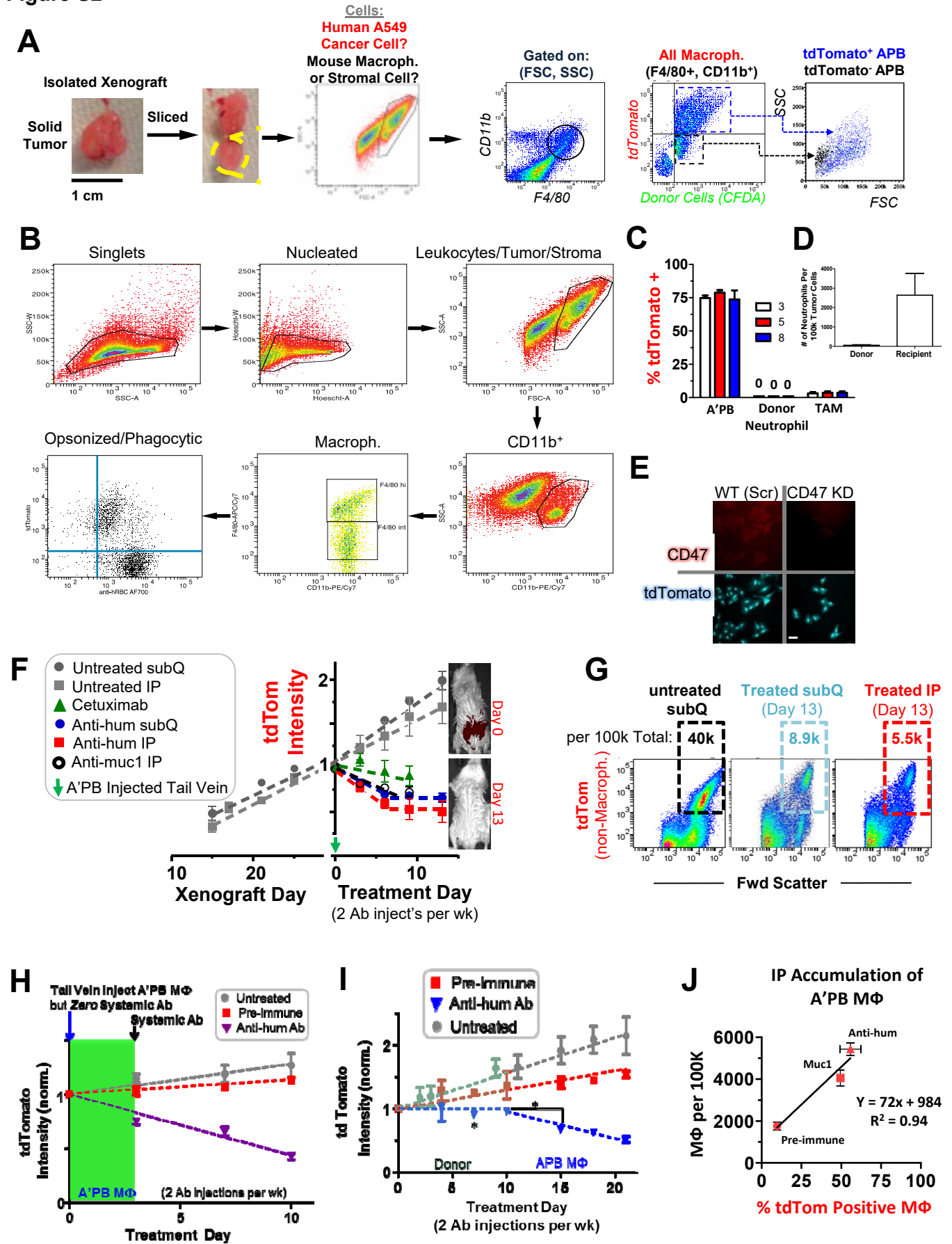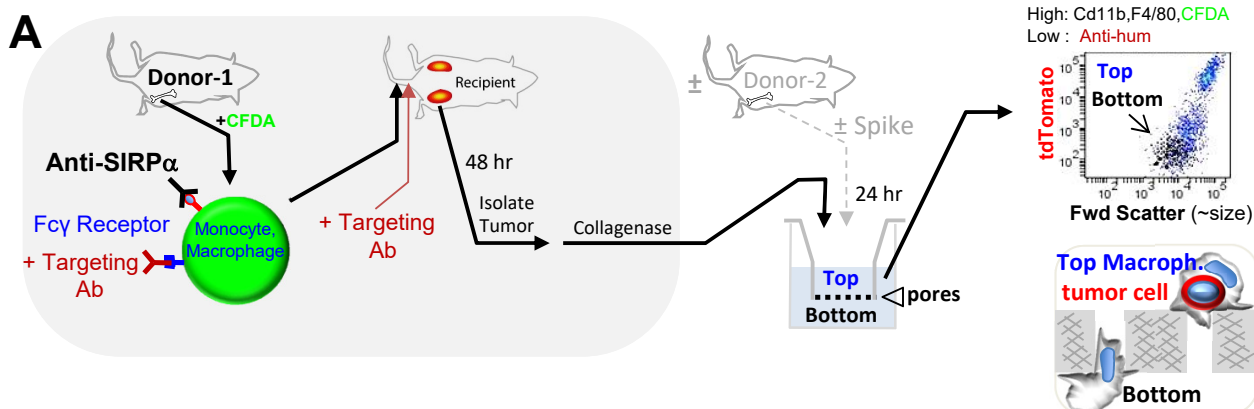
# Figure S2



**A** Isolated Xenograft

Solid Tumor → Sliced

1 cm

Cells:
Human A549 Cancer Cell?
Mouse Macroph. or Stromal Cell?

Gated on: (FSC, SSC)
CD11b / F4/80

All Macroph. (F4/80+, CD11b+)
tdTomato
Donor Cells (CFDA)

tdTomato+ APB
tdTomato- APB
SSC / FSC

**B**
Singlets — Nucleated — Leukocytes/Tumor/Stroma

Opsonized/Phagocytic — Macroph. — CD11b+

F4/80 hi
F4/80 int

**C**
% tdTomato +
A'PB   Donor Neutrophil   TAM
0 0 0
3 5 8

**D**
# of Neutrophils Per 100k Tumor Cells
Donor   Recipient

**E**
WT (Scr) | CD47 KD
CD47
tdTomato

**F**
- Untreated subQ
- Untreated IP
- Cetuximab
- Anti-hum subQ
- Anti-hum IP
- Anti-muc1 IP
- A'PB Injected Tail Vein

tdTom Intensity

Day 0
Day 13

10  20   0   10
Xenograft Day    Treatment Day
(2 Ab inject's per wk)

**G**
untreated subQ | Treated subQ (Day 13) | Treated IP (Day 13)
per 100k Total: 40k | 8.9k | 5.5k
tdTom (non-Macroph.)
Fwd Scatter

**H**
Tail Vein Inject A'PB MΦ but Zero Systemic Ab
Systemic Ab
- Untreated
- Pre-Immune
- Anti-hum Ab
tdTomato Intensity (norm.)
A'PB MΦ   (2 Ab injections per wk)
0   5   10
Treatment Day

**I**
- Pre-Immune
- Anti-hum Ab
- Untreated
td Tomato Intensity (norm.)
Donor   APB MΦ
*   *
0   5   10   15   20
Treatment Day
(2 Ab injections per wk)

**J**
IP Accumulation of A'PB MΦ
MΦ per 100K
Anti-hum
Muc1
Pre-immune
Y = 72x + 984
$R^2$ = 0.94
0   25   50   75   100
% tdTom Positive MΦ

**Figure S2. Donor cells alone inhibit tumor growth, but priming Fcγ receptor on APB macrophages yields the most effective anti-tumor response** (Related to **Figure 1**)

(**A**) Schematic of method used to analysis disaggregated tumor tissue. Following dissociation and antibody staining, samples are analyzed using flow cytometry (**STAR Methods**).

(**B**) Flow cytometry scatterplots with gating strategy used to identify and analysis macrophage eating and abundance in tissues.

(**C**) Phagocytosis assay using disaggregated tdTom A549 tumors that were treated 24 hours prior with A′PB macrophages. Cells were platted for 24 hours and analyzed by flow cytometry focusing on phagocytosis of tdTom A549 cells by A′PB macrophages, donor neutrophils, or recipient macrophages (TAMs).

(**D**) Three days after injection of APB engineered NSG mouse marrow, subcutaneous WT A549 tumor were harvest and analyzed by flow cytometry for neutrophils. Abundance of neutrophils in the tumor per $10^5$ cells screened. Despite the moderate level of neutrophil eating, the small number of neutrophils in the tumor make them an ineffective anti-tumor effector cell type. Recipient neutrophils are in high number of neutrophils in the tumor, but they are non-phagocytic.

(**E**) Fluorescent imaging of tdTom CD47 knockdown A549 compared to tdTom WT.

(**F,G**) Normalized *in vivo* growth curve of tdTom A549 subcutaneous and intraperitoneal tumors. Growth of tumors was monitors by tdTom fluorescent intensity. Tumors grew at a similar rate for 30 days then were treated with NSG A′PB macrophages. All tumors shrank comparably until days 9-13 when shrinkage plateaus (n = 3-6). (**inset**) Representative fluorescent images of tdTom signal from IP tumors comparing tumor intensities of treatment day 0 to day 13. (**G**) On Day 13, all tumors were removed and analyzed by flow cytometry. TdTom A549 cells remaining in the tumors were identified by forward scatter (size) and tdTom+, while excluding CD11b$^+$ F4/80$^+$ cells. Tumors treated with A′PB macrophages decreased A549 populations in proportion to measured florescent intensity.

(**H**) *In vivo* growth curve of subcutaneous tdTom A549 tumors. Tumor growth was measured by tdTom intensity. Tumor were approximately 70 mm$^2$ in size at the start of treatment. Male mice were treated with 10 million NSG mouse donor marrow cells that were SIRPα inhibited and Fcγ receptor pre-loaded with anti-hum or pre-immune antibody *ex-vivo* then tail vein injected back into mice. Donor injection was giving on day 0 with no systemic antibody treatment. On treatment day 3, biweekly systemic injection of antibody (n = 6).

(**I**) *In vivo* growth curve of subcutaneous WT tdTom A549 tumors. Tumor growth was measured by tdTom intensity. Tumor were approximately 70 mm$^2$ in size at the start of treatment. Treatment day 0-10 mice were injected with 10 million marrow donor cells with biweekly anti-hum injection. On day 10, a mixture of male and female mice received a second treatment donor cells, but with SIRPα inhibit. (n = 4).

(**J**) A′PB macrophages accumulation in IP tdTom A549 tumors as a function of % tdTom+ macrophages within each pollution. Relative phagocytosis and accumulation depends on the antibody used to opsonize cancer cells with the following order: anti-hum › anti-hMuc1 › Pre-immune (n = 3; R$^2$=0.94).

# Figure S3

Eng'd Donor Macrophages in Recipient Tumor are assayed for Phagocytosis and 3D-Motility

**A**



High: Cd11b,F4/80,CFDA
Low : Anti-hum

Accumulation of Macroph. is caused by Phagocytosis of Tumor Cells, which impedes 3D-Motility.

**B**



|  | Bottom tdTom+ %(Top+Bott) | |
|---|---|---|
| ■ Donor-1 Tumor A'PB | 0 | 0 |
| ○ Recipient TAM | 0 | 0 |
| A549 cells (Top: 100% tdTom+) | 3 | 7 |
| ▽ Donor-2 A'PB Spike | 0 | 8 |
| △ Donor-2 Macroph. Spike | 0 | 0 |
| ◇ Lung Macroph. | 0 | 0 |
| ✳ Donor-2 A'PB Spike | 0 | 0 |

Tumor, A549

Mouse Lung

$y = 0.17 x + 84$
$R^2 = 0.91$

$y = 0.50 x + 50$
$R^2 = 0.99$

**C**
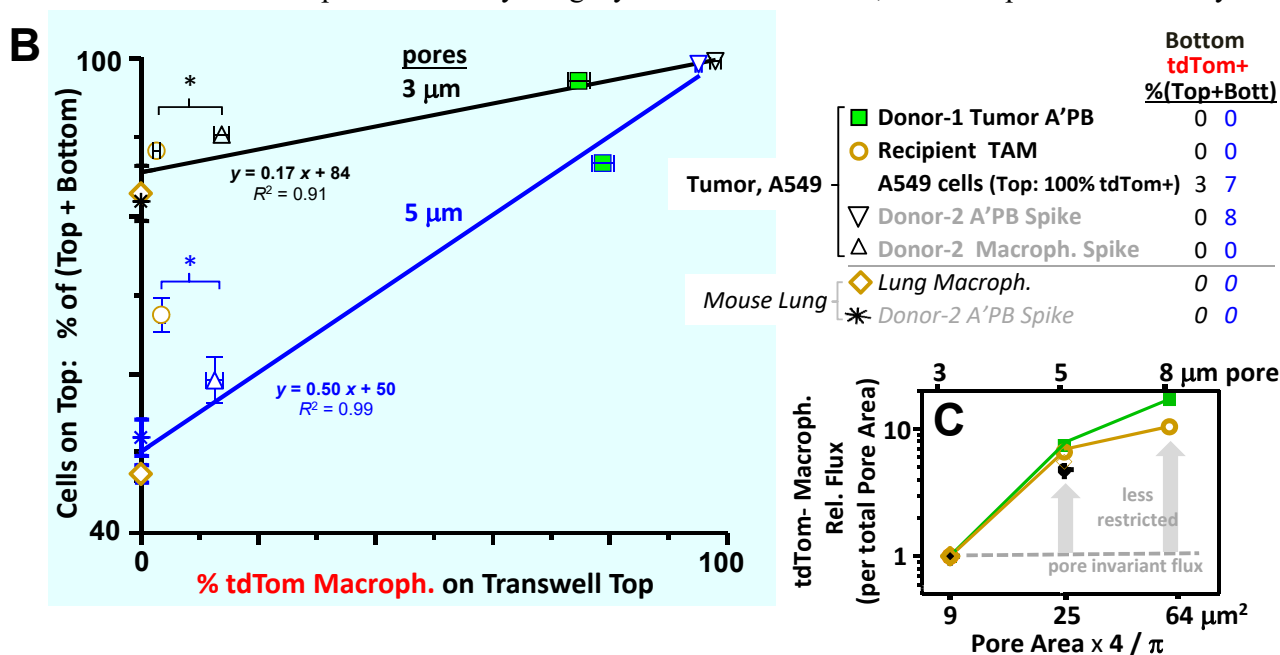
**Figure S3. Engineered donor macrophages in recipient tumors are assayed for phagocytosis and 3D-Motility** (Related to **Figure 2**)

(**A**) Schematic of the 3D-motility assay used to assess macrophage eating and migration from primary NSG mouse marrow, lung, and tdTom A549 subcutaneous tumors. Bone marrow from donor-1 was harvested, engineered (SIRPα inhibited and Fcγ receptor primed with anti-hum), and injected into NSG mice with 8 wk old subcutaneous tdTom A549 tumors on both flanks. Three days after injection a injection of anti-hum was given and 3 hours later tumors were isolated and plated on tops of 3 μm and 5 μm transwells at 300k cells per well and allowed to migrate for 24 hours. In some conditions marrow from a second donor was spiked with the disaggregated tumor. The transwells were scrapped, stained and analyzed by flow cytometry.

(**B**) Plot of 3D migration of donor marrow, lung, and tumor macrophages as a function of macrophage phagocytic activity of tdTom A549 cells on 3 μm (black) and 5 μm (blue) pores (n ≥ 3). (**inset table**) macrophage eating of tdTom A549 cells on the bottom of 3 μm (black) and 5 μm (blue) transwells along with migration of tdTom A549 tumor cells. Only one condition shows eating on bottom (most phagocytic with largest pores) (n =3 -7).

(**C**) Transwells with different pore sizes have different numbers of pores (3 μm = $2\text{x}10^6$, 5 μm = $0.4\text{x}10^6$, etc.), which must be accounted for in the total pore area to calculate cell flux (#/area). Thus the flux of cells through 5 μm pores should be smaller by $(5/3)\char`\^2(0.4\text{x}10^6/2\text{x}10^6)$ = 0.56-fold, but the 5 μm transwell instead allows 3-fold more of each macrophage phenotype through because the 5 μm constriction is far less severe than the 3 μm. The plotted flux of macrophages is therefore 5.4-fold higher for this larger pore, whereas the much larger 8 μm pore does not greatly increase this flux, so that 3 μm pores are by far the most restrictive.

## Figure S4

Recipients shrink Tumors *only* with CD47-Knockdown & with Tail Vein injection of Ab.



**A**

WT (shCtl)
CD47 KD+

Pre-Treatment

normalize

1 mm²/day

Tumor Area (mm²)

Xenograft Day

WT(shCtl)    +Ab
CD47 KD⁺    ▼+Ab

P= 0.04

P= 0.007

200 µg    600 µg Ab    No Ab injections    600 µg Ab

Treatment Day (2 Ab injections per wk)

**B**

Caliper Area (mm²)

**Total tdTom Intensity**

Treatment

**C**

KD⁺⁺    WT

CD47 KD⁺⁺
Mosaic
WT GFP (Scr)

1.56 mm²/day

1.02 mm²/day

Tumor Area(mm²)

Xenograft Day
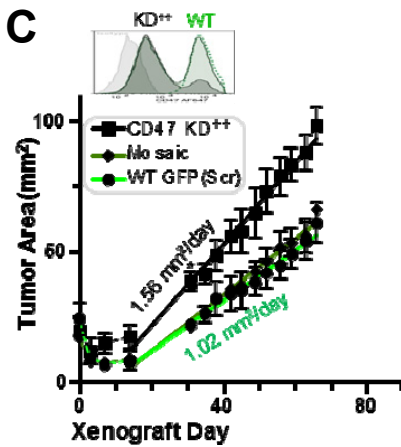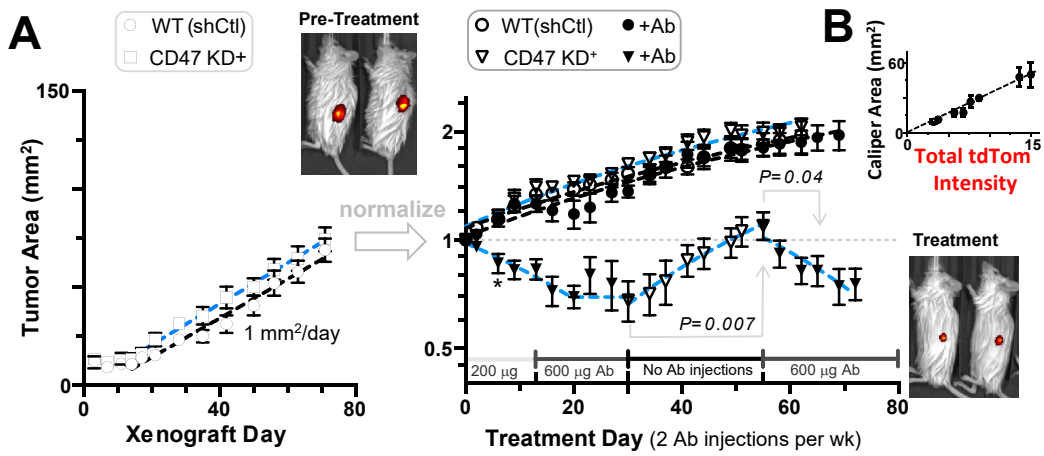
Tumor regression requires anti-mSIRPA, but a plateau is followed by normal re-growth

**D**    WT tdTom A549 in male & female mice

Untreated
pre-immune
anti-h

APB

Re-growth

+ anti-SIRPA

No anti-SIRPA

plateau

Tumor Area (Norm.)

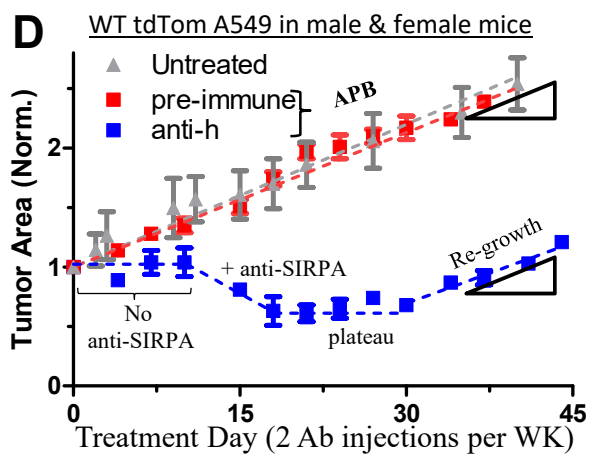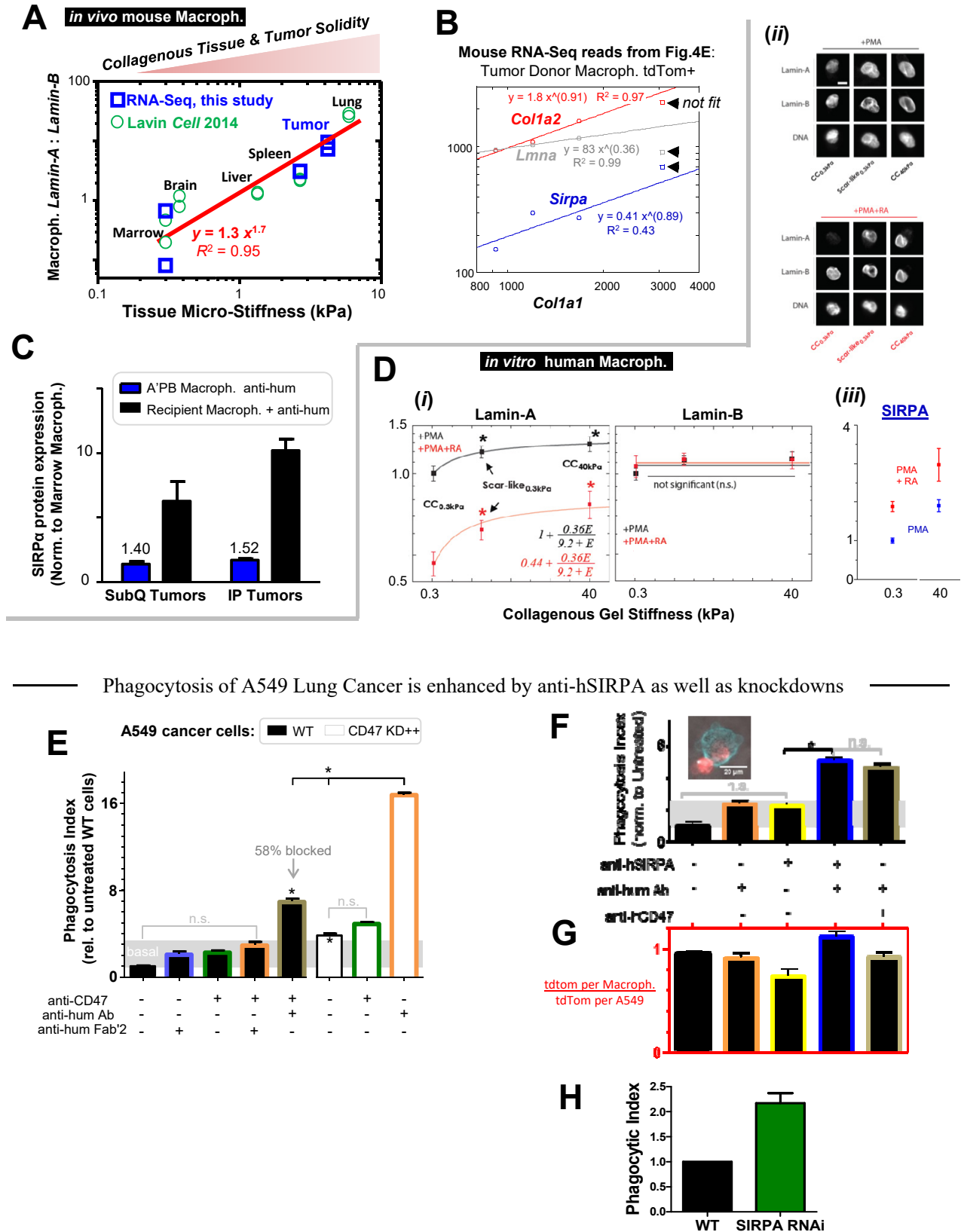Treatment Day (2 Ab injections per WK)

**Figure S4: TAM dependent shrinkage of CD47 Knockdown tumors** (Related to **Figure 3**)

(**A, Left**) *In vivo* growth curve of CD47 KD⁺ during 2 periods of no treatment. (n = 8-12). Slope of linear fit = 1.02 mm²/day corresponding to tumor growth rate ($R^2$=0.99). (**insets**) Representative fluorescent overlays of untreated (left) and Ab treated (right) mice at the end of the treatment period. (**A, Right**) Tumor response to 200 and 600 µg anti-human / mouse followed by removal of antibody and subsequent re-administration (n = 4-8).

(**B**) *In vivo* measured growth of subcutaneous tdTom A549 tumors. Correlation of measuring tumors using calipers (cross sectional area) or by tdTom intensity over a 30 day period (n = 4 mice).

(**C**) CD47 KD⁺ cells were further sorted to generate CD47 KD⁺⁺, an ultra-deep knockdown. Xenotransplants in NSG mouse flanks show a slight growth advantage for CD47 KD⁺⁺ (linear fit slope = 1.56 mm²/day, $R^2$=0.99) compared to tumors comprised of WT GFP Scr (same as WT/shCtl) either in part or in whole (linear fit slope = 1.02 mm²/day, $R^2$=0.98) (n = 4 - 8). (**inset**) Flow cytometry of cells used in xenotransplants (gray=isotype; black=CD47 KD⁺⁺; green dashed outline=WT GFP Scr; green fill=Mosaic).

(**D**) Growth kinetics of tdTom A549 tumors after 8 wks. NSG marrow cells (10M without SIRPα inhibition) were injected with anti-hum at day-0 (n = 4) followed by biweekly anti-hum injection. On day-10, the cohort of male and female mice received a second treatment donor cells but this time with SIRPα inhibition.

# Figure S5

Consistent with increased Collagen Matrix in Tumor Macroph.;
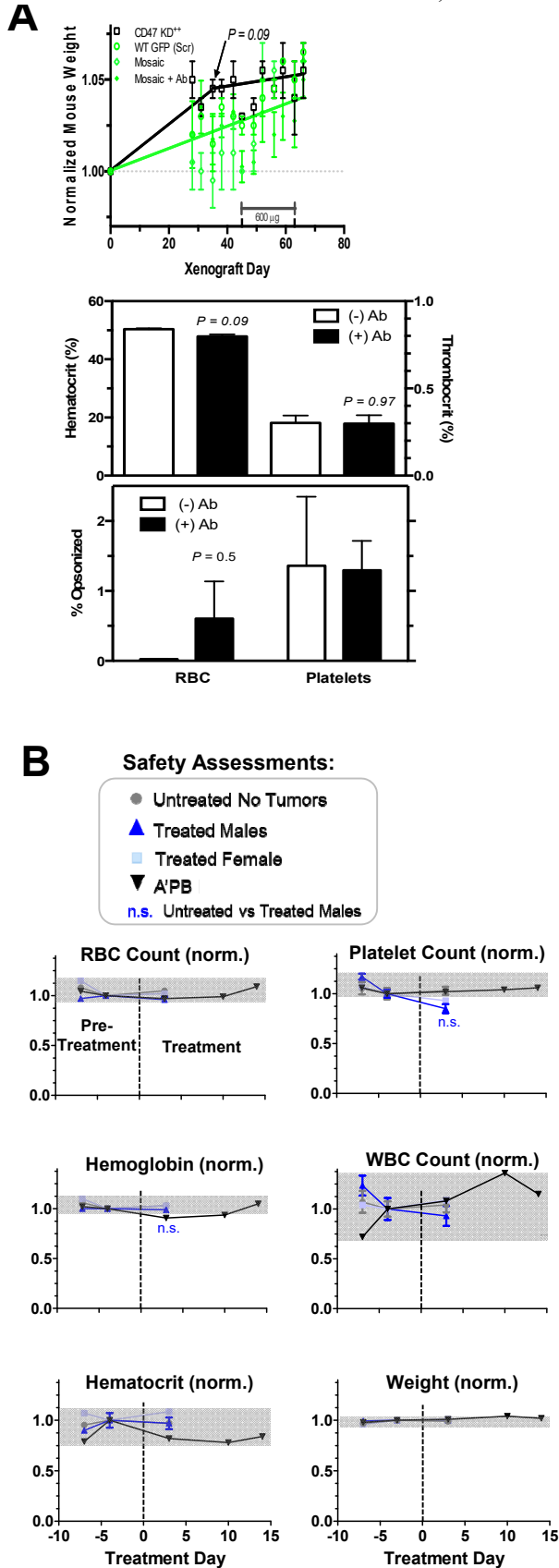Microenvironment stiffness increases nuclear Lamin-A and SIRPA message and protein

**A** *in vivo* mouse Macroph.



Collagenous Tissue & Tumor Solidity

■ RNA-Seq, this study
○ Lavin *Cell* 2014

$y = 1.3\ x^{1.7}$
$R^2 = 0.95$

Macroph. *Lamin-A : Lamin-B*

Tissue Micro-Stiffness (kPa)

Marrow, Brain, Liver, Spleen, Tumor, Lung

**B**

Mouse RNA-Seq reads from Fig.4E:
Tumor Donor Macroph. tdTom+

$y = 1.8\ x^{(0.91)}$   $R^2 = 0.97$   ◄ *not fit*
*Col1a2*

*Lmna*   $y = 83\ x^{(0.36)}$
$R^2 = 0.99$

*Sirpa*

$y = 0.41\ x^{(0.89)}$
$R^2 = 0.43$

*Col1a1*

*(ii)*



**C**

■ A'PB Macroph. anti-hum
□ Recipient Macroph. + anti-hum

SIRPα protein expression
(Norm. to Marrow Macroph.)

1.40    1.52

SubQ Tumors    IP Tumors

**D** *in vitro* human Macroph.

*(i)*

Lamin-A

+PMA
+PMA+RA

Scar-like$_{0.3kPa}$

CC$_{40kPa}$

CC$_{0.3kPa}$

$1 + \dfrac{0.36E}{9.2 + E}$

$0.44 + \dfrac{0.36E}{9.2 + E}$

Lamin-B

not significant (n.s.)

+PMA
+PMA+RA

Collagenous Gel Stiffness (kPa)

*(iii)* **SIRPA**

PMA + RA

PMA

---

Phagocytosis of A549 Lung Cancer is enhanced by anti-hSIRPA as well as knockdowns

**E**  A549 cancer cells: ■ WT  □ CD47 KD++

Phagocytosis Index
(rel. to untreated WT cells)

58% blocked

n.s.

n.s.

basal

| | | | | | | | |
|---|---|---|---|---|---|---|---|
| anti-CD47 | - | - | + | + | + | - | + | - |
| anti-hum Ab | - | - | - | - | + | - | - | + |
| anti-hum Fab'2 | - | + | - | + | - | - | - | - |

**F**

Phagocytosis Index
(norm. to Untreated)

n.s.

| | | | | | |
|---|---|---|---|---|---|
| anti-hSIRPA | - | - | + | + | - |
| anti-hum Ab | - | + | - | + | + |
| anti-rCD47 | - | - | - | - | - |

**G**

tdtom per Macroph.
tdTom per A549

**H**

Phagocytic Index

WT    SIRPA RNAi

**Figure S5. Stiff matrix regulation of SIRPα and Phagocytosis of a lung cancer cell line enhanced by inhibition of hSIRPα** (Related to **Figure 4,5**)

(**A**) *Lamin-A : Lamin-B* ratio of RNA-Seq reads for mouse Recipient macrophages show the same increasing trend with collagenous tissue or tumor stiffness as resident tissue macrophages ($R^2$=0.95) mined from published data.

(**B**) RNA-Seq reads from mouse Donor macrophages tdTom+. Three of the four samples are fit by power laws based on the criteria of almost linear scaling with a high $R^2$ fit of *col1a2* versus *col1a1*, which then shows *lmna* scales more weakly with *col1a1* as expected.

(**C**) Quantification of SIPRα protein on A'PB donor macrophages and recipient macrophages from large tdTom A549 IP and subcutaneous tumors in NSG mice. Tumors were isolated 3 days after tail-vein injection of donor cell. Data is normalized to macrophages taken from NSG marrow (n = 3).

(**D**) THP-1 expression of Lamin-A and SIRPA proteins increase *in vitro* with stiffness of collagen-coated gels, whereas Lamin-B levels do not change. Retinoic Acid (RA; for last 3 days, 1uM) causes an overall decrease in Lamin-A but causes an overall increase in SIRPA, whereas Lamin-B levels do not change. Heterogeneous "scar-like" gels have an effective stiffness of ~12 kPa based on studies of other cell types [S1].

(**E**) THP-1 phagocytosis of WT and CD47 KD A549 was measured by counting the number tdTom A549 cells per THP-1 and normalizing to control (cells only) under different eating condition (n≥3).

(**F**) THP-1 phagocytosis of A549 was measured by counting the number A549 cells per THP-1 and normalizing to control (cells only) under different eating condition (n ≥ 4). (**inset**) Image of a positive eating event with CD11b stain in green showing THP-1 and tdTom fluorescence indicating A549 cancer cell.

(**G**) Quantification of internalized tdTom fluorescent intensity of THP-1s and normalizing to tdTom intensity from uneaten A549 cells. Quantification was done from the samples taken from figure 1A (n ≥ 4).

(**H**) *In vitro* phagocytosis assay using PMA treated THP-1s and human red blood cells. KD of SIRPα in THP-1s resulted in 2.2-fold increase in eating of anti-hum opsonized RBCs over WT THP-1s (n = 4).

# Figure S6

## A
Blood & Weight remain in Normal Range after anti-hum Ab or various NSG donor treatments,



CD47 KD$^{++}$
WT GFP (Scr)
Mosaic
Mosaic + Ab

$P = 0.09$

600 µg

Normalized Mouse Weight
Xenograft Day

(-) Ab
(+) Ab

$P = 0.09$
$P = 0.97$

Hematocrit (%)
Thrombocrit (%)

(-) Ab
(+) Ab

$P = 0.5$

% Opsonized
RBC          Platelets

## B

**Safety Assessments:**

- Untreated No Tumors
- ▲ Treated Males
- Treated Female
- ▼ A'PB
- n.s. Untreated vs Treated Males

RBC Count (norm.)
Pre-Treatment   Treatment

Platelet Count (norm.)
n.s.

Hemoglobin (norm.)
n.s.

WBC Count (norm.)

Hematocrit (norm.)

Weight (norm.)

Treatment Day
Treatment Day

## C
Human Marrow shrinks CD47 KD A549 tumors almost as well as SIRPA-inhibited Human APB

Note: Mφ = Macroph.



tdTomato Intensity (norm.)
Treatment Day (2 Ab injections per wk)

▲ Untreated
● hDonor + Ab
■ APB hMφ

## D
% td Tomato$^+$ Mφ
hAPB Mφ    hdonor Mφ

## E
# of A549 per hMφ
hAPB Mφ    hdonor Mφ

## F
# of Mφ per 100k tumor cells
hAPB Mφ    hdonor Mφ

## G
Cumulative Phagocytosis Index
hAPB Mφ    hdonor Mφ
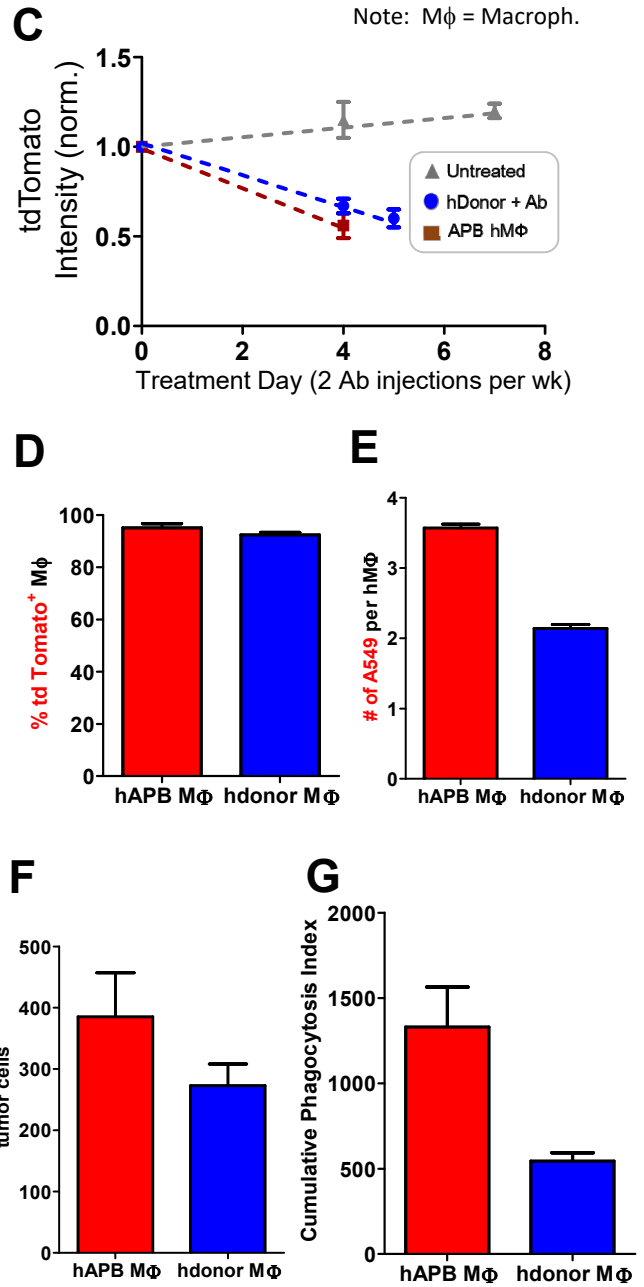
**Figure S6. Safety and *in vivo* confirmation of human donor efficacy** (Related to **Figure 1,3,6,7**)

(**A**) Weight throughout duration of study (including pre-treatment, treatment, and post-treatment). Weight is normalized to weight at date of xenograft implantation. Mice used in Mosaic Study (n = 4-8). GFP WT/shCtl, Mosaic, Mosaic+Ab are grouped together and the green solid line reflects the linear fit. CD47 KD$^{++}$ mice show slightly different weight responses as shown by the black solid line. Addition of antibody shows a slight decrease in hematocrit, but no change in thrombocrit (n ≥ 3). I.V. injection of anti-hum antibody shows no specific binding to mouse RBC or platelets *in vivo* (n ≥ 3 per group).

(**B**) Blood profiles taken from male mice treated with APB macrophages (n ≥ 3) before and after treatment. Parameters were normalized to day 4 of pre-treated.

(**C**) *In vivo* growth curve of CD47 KD tdTom A549 tumors treated with NSG donor cells and anti-hum antibody. Growth was measured by tdTom fluorescent intensity. Tumor grew for 8 wks before treatment with human marrow. SIRPα inhibition didn't significantly increase anti-tumor effect in CD47 KD tumors (n = 3).

(**D**) Quantification of CD14$^+$ CD33$^+$ CD66b$^-$ human macrophages eating in CD47 KD A549 tumors. Three days after injection tumors were harvested and human macrophages were analyzed by flow cytometry. Macrophages ± SIRPα inhibit had the same eating percentage, 95% (n = 4).

(**E**) However, human macrophages with anti-hSIRPα had engulfed an average of 3.5 tdTom A549 tumor cells whereas donor only was only 2.2 (n = 4).

(**F**) Quantification of the number of human macrophages per 10$^5$ cells screened on the flow cytometer (n = 4).

(**G**) Calculation of the cumulative phagocytosis index using data from Fig.S8D-F. The human APB macrophages indexes are comparable to indexes from NSG APB macrophages from figure 1.

**Supplemental References**

S1. Dingal, D.P., Bradshaw, A.M., Cho, S., Raab, M., Buxboim, A., Swift, J., Discher, D.E. (2015). Fractal heterogeneity in minimal matrix models of scars modulates stiff-niche stem-cell responses via nuclear exit of a mechanorepressor. Nature Materials *14*, 951-960

| | Total IgG | Adult mouse | | Ab Injections |
|---|---|---|---|---|
| | mg/mL | Blood (mL)[1] | mg IgG | % of IgG |
| C57BL/6[2] | 1.5 | 2.4 | 3.6 | 17% |
| Humanized NSG[3] | 0.165 | 2.4 | 0.4 | 154% |
| | | | | |
| | | Adult Human | | 0.3 mg Rhogam |
| | mg/mL | Blood (mL) | mg IgG | % of IgG |
| Hu Serum | 10 | 5000 | 50000 | 0.0006% |

**Table S1. Relative IgG Supplementation** (Related to **Figure 1**)
Calculated estimate of the IgG percent in immunocompetent mouse strains. Calculation assumes a 30 g mouse and 0.6 mg Ab injection. % of IgG is calculated as 0.6 mg injected Ab / total mg IgG * 100%. This value provides a magnitude of the Ab dosage for comparison with what is present in immuncompetent animals. Also as a comparison, a typical 300 µg dose of Rhogam represents 0.0006% of total human IgG. Literature values: mouse blood volume[1] from, C57BL/6 IgG concentration[2] from, humanized NSG IgG concentration[3] from.

| Cell Type | Tumor Location | per 100K Cells |
|:---:|:---:|:---:|
| A'PB MΦ | Periphery | 2921 |
| A'PB MΦ | Periphery | 3122 |
| TAM | Periphery | 3348 |
| TAM | Periphery | 3599 |
| A'PB MΦ | Core | 3399 |
| A'PB MΦ | Core | 1631 |
| TAM | Core | 6118 |
| TAM | Core | 5682 |

Note: MΦ = Macroph.

**Table S2. Donor vs TAM abundance in tumor periphery and core** (Related to **Figure 1**)
Flow cytometry population analysis of A'PB macrophages and TAMs in periphery and core of tdTom A549 subcutaneous xenografts in NSG mice.

| | | Area (µm²) | In Vitro | | In Vivo | |
|---|---|---|---|---|---|---|
| | | | CD47 (norm) | CD47/µm² | CD47 (norm) | CD47/µm² |
| | WT Scr | | 5.00±0.04 | 463 | 5.5±0.2 | 509 |
| | CD47 KD[+] | | 2.12±0.05 | 196 | 4.1±0.1 | 379 |
| | CD47 KD[++] | 382 | 1.26±0.04 | 117 | 2.37±0.07 | 219 |
| | GFP[+], CD47hi | | 6.20±0.02 | 574 | 3.9±0.2 | 361 |
| Mosaic | GFP[-], CD47hi | | 4.73±0.03 | 438 | 2.7±0.2 | 250 |
| | GFP[-], CD47lo | | 0.41±0.05 | 38 | 0.66±0.03 | 61 |
| | hRBC | 141±3.0 | 1.00 | 250 | | |

Engstrom 1998  Tsai 2008

**Table S3. CD47 Cell Surface Density** (Related to **Figure 1**)
*In vitro* (cells used for xenotransplant) and *in vivo* (cells recovered from excised tumors) CD47 surface density determined by flow cytometry and immunofluorescence. A549 cell area was determined by measuring area of well spread cells imaged by immuno-fluorescence. This value was multiplied by two assuming negligible height for well spread cells. We acknowledge that this method underestimates cell area and calculated values for CD47/µm² are thus likely overestimates. CD47 intensity was determined by flow cytometry mean fluorescence intensity and normalized to human red blood cells. Arrows indicate IgG treatment responsive cells. We previously reported a CD47 surface density value for hRBCs. Multiplying this value by the normalized CD47 intensity and scaling by the ratio of A549 area to hRBC area previously reported, results in the values presented in the table.

| | | MHC II (M1-type MΦ) | | | | | | CD206 (M2-type MΦ) | | | | | | Mean M1/M2 |
|---|---|---|---|---|---|---|---|---|---|---|---|---|---|---|
| | *Replicate* | 1 | 2 | 3 | 4 | 5 | 6 | 1 | 2 | 3 | 4 | 5 | 6 | |
| **Tumor MΦ tdTom⁺** | Donor + Ab | 1706 | 1834 | 1008 | 1197 | | | 157 | 201 | 152 | 154 | | | 8.6 |
| | APB MΦ | 1371 | 1297 | 1986 | 2189 | | | 276 | 191 | 308 | 257 | | | 6.7 |
| | Recipient | 1201 | 1181 | | | | | 1147 | 567 | | | | | 1.6 |
| | Recipient + Ab | 1235 | 1125 | 1255 | 1213 | 1000 | 1024 | 852 | 667 | 582 | 636 | 384 | 366 | 2.1 |
| **Tumor MΦ tdTom⁻** | Donor + Ab | 1892 | 1534 | 1320 | 1354 | | | 183 | 625 | 226 | 250 | | | 6.0 |
| | APB MΦ | 1564 | 1355 | 2414 | 1867 | | | 230 | 670 | 729 | 606 | | | 3.8 |
| | Recipient | 87 | 80 | | | | | 10759 | 5665 | | | | | 0.01 |
| | Recipient + Ab | 252 | 331 | 1194 | 786 | 414 | 240 | 9085 | 10299 | 12362 | 6789 | 11001 | 4342 | 0.06 |
| **Marrow MΦ tdTom⁻** | Donor + Ab | 1690 | | | | | | 620 | | | | | | 2.7 |
| | APB MΦ | 447 | 784 | | | | | 103 | 60 | | | | | 8.7 |
| | Recipient | 301 | | | | | | 293 | | | | | | 1.0 |
| | Recipient + Ab | 2200 | 298 | | | | | 160 | 47 | | | | | 10.1 |
| **Spleen MΦ tdTom⁻** | Donor + Ab | 451 | | | | | | 355 | | | | | | 1.3 |
| | APB MΦ | | | | | | | | | | | | | |
| | Recipient | | | | | | | | | | | | | |
| | Recipient + Ab | 806 | | | | | | 913 | | | | | | 0.9 |
| **Liver MΦ tdTom⁻** | Donor + Ab | 342 | | | | | | 224 | | | | | | 1.5 |
| | APB MΦ | | | | | | | | | | | | | |
| | Recipient | | | | | | | | | | | | | |
| | Recipient + Ab | 64 | | | | | | 2048 | | | | | | 0.03 |

Note: Mφ = Macroph.   ▨ not measured

**Table S4. Marrow macrophages in Tumors can maintain M1 marker** (Related to **Figure 4**)
Donor and recipient macrophages isolated from different tissues 2-3 days after cell injections were stained for M1 (MHC II) and M2 (CD206) markers. Donor macrophages in tumor exhibit strong M1>M2 surface markers (arrows) regardless of phagocytic activity. Recipient macrophages show: (*i*) strong M1>M2 only in marrow after Ab injection, and (*ii*) weak M1>M2 only in tumor when phagocytic.